

Visceral pleural invasion by pulmonary adenocarcinoma ≤ 3 cm: the pathological correlation with pleural signs on computed tomography

Shuyi Yang^{1,2,3#}, Liang Yang^{4#}, Lin Teng^{2,3,5}, Shan Zhang^{2,3}, Yue Cui^{2,3}, Yukun Cao^{2,3}, Heshui Shi^{2,3}

¹Department of Radiology, Shanghai Public Health Clinical Center, Fudan University, Shanghai 201508, China; ²Department of Radiology, Union Hospital, Tongji Medical College, Huazhong University of Science and Technology, Wuhan 430022, China; ³Hubei Province Key Laboratory of Molecular Imaging, Wuhan 430022, China; ⁴Department of Orthopaedics, Union Hospital, Tongji Medical College, Huazhong University of Science and Technology, Wuhan 430022, China; ⁵Department of Radiology, Henan Provincial People Hospital, Zhengzhou 450000, China

Contributions: (I) Conception and design: S Yang, L Yang, H Shi; (II) Administrative support: H Shi; (III) Provision of study materials or patients: S Yang, L Yang, H Shi; (IV) Collection and assembly of data: S Yang, L Yang, L Teng, S Zhang, Y Cui, Y Cao; (V) Data analysis and interpretation: S Yang, L Teng, S Zhang, Y Cui, Y Cao; (VI) Manuscript writing: All authors; (VII) Final approval of manuscript: All authors.

[#]These authors contributed equally to this work.

Correspondence to: Heshui Shi. Department of Radiology, Union Hospital, Tongji Medical College, Huazhong University of Science and Technology, Wuhan 430022, China; Hubei Province Key Laboratory of Molecular Imaging, Wuhan 430022, China. Email: heshuishi@hotmail.com; heshuishi@hust.edu.cn.

Background: (I) To categorize and quantitatively analyze pleural signs on CT of pulmonary adenocarcinoma (≤ 3 cm); (II) to evaluate the association between pleural signs and visceral pleural invasion (VPI) of adenocarcinoma.

Methods: The clinical data of 52 pulmonary adenocarcinoma patients with 91 involved pleurae were retrospectively analyzed in one single institution. Pleural signs were categorized into five types of non-interlobar fissure pleura (group A) and four types of interlobar fissure pleura (group B). A new parameter called pleural indentation fraction (PIF) was firstly defined to quantitatively evaluate the level of pleural shift.

Results: In group A, type I pleural sign accounted for 15.79%, type II for 31.58%, type III for 21.05%, type IV for 10.53%, type V for 21.05%. The PIF of type II–III was 0.494 ± 0.204 . In group B, type I accounted for 67.65%, type II for 14.71%, type III for 8.82%, type IV for 8.82%. The PIF of type I was 0.188 ± 0.083 , significantly different with type II–III of group A ($t = -7.444$, $P < 0.001$). The PIF of type I in group B had significant linear correlation with the tumor distance to the primary pleura. 41 patients with 75 involved pleurae formed the study part of pathological correlation with pleural signs. The rate of VPI was 87.5% (type III), 80% (type IV) in group A and 84.2% (type I), 40% (type II) in group B ($t = 30.895$, $P < 0.001$). The ratio of type III in group B was 2/2. Four cases with non-intact extrapleural fat layer were pathologically confirmed with VPI in type IV of group A. Six of seven cases with mediastinal pleural abnormality (type II–IV) were confirmed with VPI.

Conclusions: Pleural signs can be categorized into five types of group A and four types of group B in the study. Type III–IV of group A and type I and III of group B may be indicators to VPI. Non-intact extrapleural fat layer and mediastinal pleural abnormality may increase the diagnosis accuracy of VPI.

Keywords: Visceral pleural invasion (VPI); computed tomography (CT); pleural signs; pathology

Submitted Dec 18, 2017. Accepted for publication Jun 11, 2018.

doi: 10.21037/jtd.2018.06.125

View this article at: <http://dx.doi.org/10.21037/jtd.2018.06.125>

Introduction

Lung cancer is one of the most life-threatening diseases in the world with high morbidity and mortality (1). Non-small cell lung cancer (NSCLC) accounts for 85% of lung cancers (2). Pulmonary adenocarcinoma mainly locates in the peripheral lung field which may result in pleural invasion. Pleural invasion, which is pathologically confirmed, is an important staging indicator and prognosis factor. Visceral pleural invasion (VPI) is defined as the tumor that extends to the elastic layer of visceral pleura but not beyond the visceral pleural surface (3,4). If the tumor (≤ 3 cm) is confirmed with VPI, the TNM upstages to T2 (3). Many scholars found VPI could be an independent risk factor of poor prognosis (4-6). One of the most well-concerned pleural signs on CT is pleural indentation (PI) which can be an indicator to the malignant lesion (7). Hsu *et al.* categorized pleural tags into 3 types and firstly evaluated the association of pleural tags with VPI of NSCLC that did not about the pleural surface (8).

The recent study of interlobar pleural signs of pulmonary adenocarcinoma on CT and the correlation between pleural signs with VPI is scarce. Preoperative diagnosis of VPI is difficult but vital for tumor staging, which can be used to guide therapy selection and improve prognosis. In this research, we will categorize and quantitatively analyze pleural signs on CT of pulmonary adenocarcinoma (≤ 3 cm), and evaluate the association between pleural signs and pathologically confirmed VPI of adenocarcinoma.

Methods

Patients

The review board of Tongji Medical College, Huazhong University of Science and Technology approved the protocol of this study (No. S254) and waived the requirement for patient informed consent.

Clinical data were retrospectively reviewed, including pathological records and CT findings of patients with pulmonary adenocarcinoma treated in our institution from September, 2014 to March, 2017. The inclusion criteria were as follows: (I) tumor size was smaller than 3 cm, (II) distance from tumor to chest wall was smaller than 3 cm, (III) without other severe lung diseases such as atelectasis, infection, pleural effusion, etc. The exclusion criteria were (I) ill-defined clinical data including unclear CT findings or incomplete pathological records, (II) the duration between CT imaging and subsequent surgery was more

than 2 weeks.

Fifty-two patients, including 31 males and 21 females aged from 40 to 77 years (median age 58 years) formed this review. Of these, 41 patients underwent tumors resection with pathological record of the tumor extent, and 11 patients underwent needle biopsy.

Pathology

All the resected tumors (pathologically stained by Hematoxylin and Eosin) with their involved pleurae (masstone stain) were evaluated by microscopic specimen in the slice thickness of 0.5 cm. The specific elastic stain was performed if the elastic layer of involved visceral pleura was unclear. Pleural invasion was staged according to the 8th edition of the TNM staging system as following:

- ❖ P10, without pleural involvement or reaching the visceral pleural connective tissue beneath the elastic layer;
- ❖ P11, extending beyond the visceral pleural elastic layer without exposing on the surface;
- ❖ P12, exposing on the visceral pleural surface without involving the parietal pleura;
- ❖ P13: parietal pleura involved (3).

P11 or P12 indicates VPI.

CT imaging

Patients underwent conventional thoracic CT examinations using a multi-slice spiral computed tomography scanner (Somatom Definition AS+, Siemens Healthineer, Germany) in our institution. Scanning range was from the level of thoracic inlet to the inferior level of costophrenic angle. The CT parameters were as follows: detector collimation width, 128×1.5 mm; pitch, 1.2; tube voltage, 120 kV; tube current was timely adjusted by the automatic exposure control system (CARE Dose 4D). Image thickness and interval were 5 and 5 mm; matrix, 512×512. Nonionic iodinated contrast agent (60–80 mL iohexol 350 mgI/mL, Beilu Pharmaceutical Co., Ltd.; Beijing, China) was injected from cubital vein at the dose of 3 mL/s in 35 patients. Thin-slice reconstruction (1.5 mm) and image post-processing were conducted after scanning.

Pleural signs analysis on CT

All the reconstructed thin-slice images were sent to the Picture Archiving and Communication System (PACS).

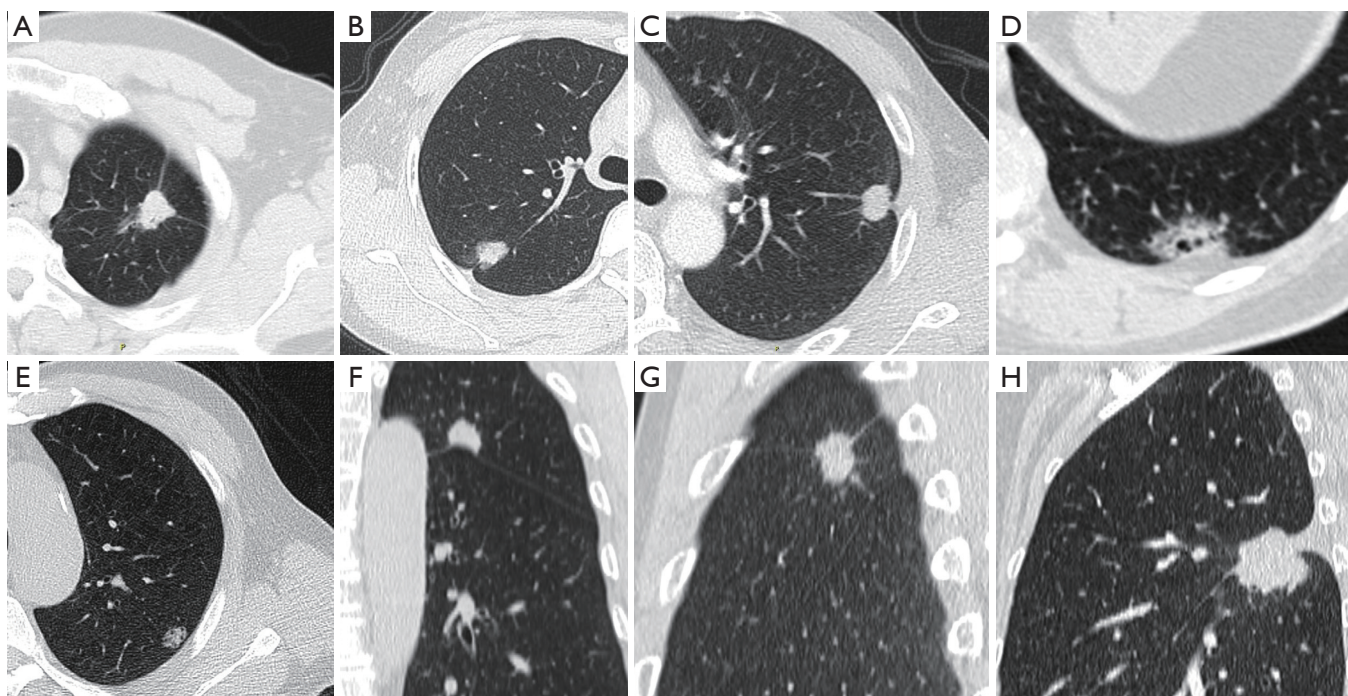


Figure 1 Pleural signs on CT. (A) type I of group A, two linear pleural tags on the lung window; (B) type II of group A, one linear pleural tag with soft tissue component at the pleural end; (C) type III of group A, one cord-like pleural tags with soft tissue component at the pleural end; (D) type IV of group A, tumor about the pleura; (E) type V of group A, without pleural abnormality; (F) type I of group B, tumor pulls pleura with pleural shift; (G) type II of group B, one or more linear pleural tags without pleural shift; (H) type III of group B, tumor push pleura.

The images could clearly show the tumor location, density and size in proper window width and level by the reference standards of 1,000 and -400 Hu. Pleural signs were categorized into five types of non-interlobar fissure pleura and four types of interlobar fissure pleura (*Figure 1*).

For non-interlobar fissure pleura (Group A): type I, one or more linear pleural tags without pleural thickened; type II, one or more linear pleural tags with soft tissue components at the pleural end; type III, one or more bold-wire pleural tags with soft tissue components at the pleural end; type IV, tumor abutting the pleura; type V, without pleural abnormality. For interlobar fissure pleura (Group B): type I, tumor pulls pleura with pleural shift; type II, one or more linear pleural tags without pleural shift; type III, tumor pushes pleura; type IV, without pleural abnormality. They should be prioritized into type III, II and I of group A when more than one type were present. Extrapleural fat layer of type IV in group A was evaluated in this study. A new parameter, called pleural indentation fraction (PIF), was defined as the ratio of pleural shift distance to the projected length of involved pleura to quantitatively evaluate the level

of pleural shift (*Figure 2*). The analysis of CT findings was performed independently by two senior radiologists with 10-year reading experience. If disagreement occurred, the readers discussed it and reached a consensus.

Statistical analysis

All data were analyzed by using a statistical software (SPSS version 22.0). The descriptive analysis for tumor location, size, density and pleural signs were performed. Levene test was performed to test the data distribution, and then independent-sample *t*-tests were performed to evaluate the relationship of tumor distance to pleura between type I with II of group B and that of the PIF value between group A with B. Durbin-Watson autocorrelation test was performed, and then linear regression was performed to analyze the relationship of PIF with tumor size and tumor distance to pleura. Chi-square test (Fisher exact test) and descriptive analysis were performed to evaluate the association of pleural signs with VPI. A P value less than 0.05 was indicative of statistical significance.

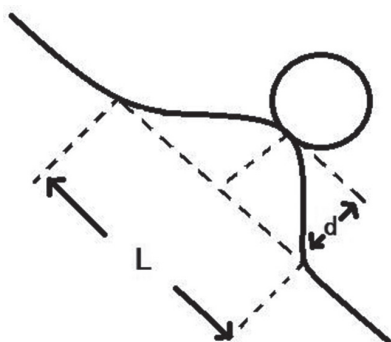


Figure 2 Diagram of PIF calculation, 'L' represents the projected length of involved pleura, 'd' represents the pleural shift distance. $PIF = d/L$. PIF, pleural indentation fraction.

Table 1 The essential features of tumors

Characteristics	Number*
Left lung	
Superior lobe	17 [14]
Inferior lobe	4 [4]
Right lung	
Superior lobe	17 [10]
Middle lobe	7 [7]
Inferior lobe	7 [6]
Non-interlobar fissure pleura	
Costal pleura	44 [35]
Mediastinal pleura	11 [9]
Diaphragmatic pleura	2 [2]
Interlobar fissure pleura	
Oblique fissure pleura	24 [21]
Horizontal fissure pleura	10 [8]
Density	
Solid	40 [29]
Non-solid	12 [12]

*, the number inside the [] is the quantity of resected lesions.

Results

Pleural signs on CT

There were 52 patients with 52 pulmonary adenocarcinoma (≤ 3 cm) in this study. Of these, 21 (40.38%) were located in the left lung and 31 (59.62%) were in the right lung.

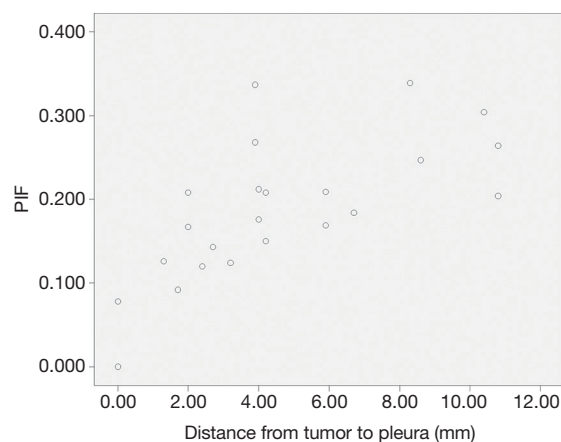


Figure 3 The scatter diagram of PIF value and tumor distance to involved pleura. The distribution of dots shows the linear correlation. PIF, pleural indentation fraction.

The number of tumors located in the superior lobes was 34 (65.38%). The mean tumor size was 2.20 ± 0.63 cm (range, 1.0–3.0 cm). There were 91 involved pleurae in this study (Group A: 57, Group B: 34) (Table 1).

In group A, the number of type I pleural sign was 9 (15.79%), type II 18 (31.58%), type III 12 (21.05%), type IV 6 (10.53%), type V 12 (21.05%). The PIF value of type II–III with pleural shift was 0.494 ± 0.204 (PIFmax = 1, PIFmin = 0.233). Five of six involved pleurae of type IV were showed with non-intact extrapleural fat layer. There were eleven involved mediastinal pleurae in this study (type II, 4; type III, 3; type IV 1, type V, 3). In group B, the number of type I pleural sign was 23 (67.65%), type II 5 (14.71%), type III 3 (8.82%), type IV 3 (8.82%). The tumor distances to interlobar pleura of type I and II were 4.65 ± 3.27 and 9.66 ± 6.42 mm ($t = -2.588$, $P = 0.016$), respectively. The values of distance were normally distributed, and that of type II was the bigger. The PIF of type I in group B was 0.188 ± 0.083 (PIFmax = 0.339, PIFmin = 0). Compared with type II–III of group A ($t = -7.444$, $P < 0.001$), the values were abnormally distributed and smaller than group A. The PIF of type I in group B had no significant linear correlation with the tumor size, but with significant linear correlation with the tumor distance to the primary pleura (Figure 3). The parameters of the model had no autocorrelation and the Pearson correlation coefficient was 0.682 ($P < 0.001$). The equation of linear regression was $y = 0.108 + 0.017x$ ('y' represents PIF value, 'x' represents tumor distal distance to pleura, $P < 0.001$) and with statistical significance (Table 2).

Table 2 The parameter of linear regression equation

Equation of linear regression	Unstandardized coefficient		Standardized coefficient	t	Sig.
	B	Standard error			
Constant	0.108	0.023	–	4.766	0.000
Distance from tumor to pleura mm	0.017	0.004	0.682	4.276	0.000

Table 3 The features of pleural signs

Group	Type	Number of involved pleurae (total/resected)	Value of PIF	Extrapleural fat layer (intact/not intact)	Rate (ratio) of VPI (%)
A	I	9/8	–	–	0
	II	18/15	0.494±0.204 (PIFmax =1, PIFmin =0.233)	–	66.7
	III	12/8	–	–	87.5
	IV	6/5	–	1/5	80
	V	12/10	–	–	0
B	I	23/19	0.188±0.083 (PIFmax =0.339, PIFmin =0)	–	84.2
	II	5/5	–	–	40
	III	3/2	–	–	2/2
	IV	3/3	–	–	0/3

PIF, pleural indentation fraction; VPI, visceral pleural invasion.

Pathological correlation with pleural signs

Forty-one patients with 75 involved pleurae formed this part of the study [Group A: type I, 8 (17.39%); type II, 15 (32.61%); type III, 8 (17.39%); type IV, 5 (10.87%); type V, 10 (21.74%); Group B: type I, 19 (65.52%); type II, 5 (17.24%); type III, 2 (6.90%); type IV, 3 (10.34%)]. The rate of VPI was 0 (type I), 66.7% (type II), 87.5% (type III), 80% (type IV) in group A and 84.2% (type I), 40% (type II) in group B. The Fisher exact test value was 30.895 ($P < 0.001$). The rate difference of VPI of pleural signs was statistically significant, while the number of lesions in type III and IV of group B was too small to be in the test with the ratio 2/2 and 0/3. Four cases with non-intact extrapleural fat layer were pathologically confirmed with VPI in type IV of group A, while another one with intact extrapleural fat layer without VPI. Six of seven cases with mediastinal pleural abnormality (type II–IV) were confirmed with VPI, while two other cases without mediastinal pleural abnormality (type V) were all confirmed without VPI. The PIF of type I in group B had no correlation with VPI (Table 3).

The part of the involved pleurae with tumors resection showed PI in the gross specimen during and after the

operation. When the tumors were sectioned perpendicular by the pleura, the involved pleura showed indenting to the tumor with unclear boundary (Figure 4).

Discussion

The pleural signs were categorized into nine types according to the involved pleural morphological changes. Of these, type I–III of group A and type I–II of group B are different forms of PI, which were also called as pleural retraction sign and pleural tags. PI was firstly discovered by Simon in 1962 and subsequently comprehensively depicted by Rigler in 1965 (7,9,10). Some scholars found that the causes of PI were associated with intratumor fibrosis and tumor distance to chest wall (11), which could be the factors for different forms of PI in group A and B.

A new radiological parameter called PIF was defined to quantitatively evaluate the extent of pleural shift. In our study, the PIF value in group A was bigger than that in group B which was resulted from the structure features of different pleurae. Non-interlobar fissure pleura consisted of visceral pleura, pleural cavity and parietal pleura which



Figure 4 Pleural indentation in the gross specimen. (A) The involved pleura indents to the tumor (white arrow) in gross specimen; (B) tumor sectioned perpendicularly, the involved pleura indents to the tumor (white arrow head, white arrow point to the tumor); (C) the slice of specimen, pleura stained by masstone and indents to tumor (black arrow).

was fixed on the chest wall, but interlobar fissure pleura consisted of bilayer visceral pleura which was mostly surrounded by aerated pulmonary tissue. When the tumor pulled the visceral pleura of non-interlobar pleura, the negative pressure of pleural cavity increased so as to restrict the movement of visceral pleura especially in the lateral direction. If tumor pulled visceral pleura of interlobar pleura, the aerated pulmonary tissue wasn't stable, resulting in the broad pleural shift. The PIF value had no correlation with tumor size but with significant linear correlation with tumor distance to pleura in type I of group B. We could estimate the PIF value according to the tumor distance by the equation of linear regression. The tumor pushed interlobar pleura with pleural shift was sometimes difficult to be differentiated from tumor growth across the fissure.

According to the golden standard of pathological records, pleural invasion is divided into four stages while VPI is defined as P11 or P12 (3,12). When the lung cancer (≤ 3 cm) is accompanied by VPI in group A, the TNM upstages to T2 (3). But it is still controversial to stage the tumor with VPI in group B. Some researchers proposed staging to T2 which was in accordance with the Japanese lung cancer society (13,14), while some other researchers proposed staging to T3 according to the prognosis (15). In a word, it is important but difficult to evaluate the presence of VPI preoperatively.

In our study, the involved pleurae of type III were with the highest rate of VPI (87.5%) in group A followed by type IV and II. All the involved pleurae of type I in group A were

confirmed without VPI. The pathologies of pleural tags are lymphatic edema for obstruction, cancer cells infiltration along lymph vessels or inflammatory cells infiltration and fibration (8). The pleural tags in type III showed thickener and unclearer which may indicate the presence of tumor cells infiltration and obstruction result in lymphatic edema, and then generates VPI. The involved pleurae of type IV in group A were also confirmed with high rate of VPI, especially with non-intact extrapleural fat layer which may predict the presence of VPI. But it may also confirm with VPI when the tumor presented with intact extrapleural fat layer in previous study (16). The involved pleurae of type I in group B were also with a high risk of VPI (84.2%) which can be an indicator to the presence of VPI. But the value of PIF had no significant correlation with VPI. Two tumors with type III pleural sign in group B were all confirmed with VPI, which may be an indicator to VPI but should be verified by more cases. On the other hand, it is difficult to clinically and pathologically assess the tumor involvement of adjacent lobes which is vital to the tumors' staging. The anatomic variation of interlobar fissure, which includes incomplete interlobar fissure (17) or fusion of the adjacent lobes (18), makes it even harder. Craig *et al.* proposed a classification of the pulmonary fissures to guide the clinical process according to the pleural variation (19). Some scholars found that reactive pleurisy rarely involved mediastinal pleura, so that the mediastinal pleural abnormality mainly prompts the presence of

malignant lesions (20). In our study, six of seven patients with mediastinal pleural abnormality were confirmed with VPI while two other patients without mediastinal pleural abnormality were confirmed without VPI. The mediastinal pleural abnormality (exclude type V of group A) may increase the accuracy of the diagnosis of VPI.

There still existed some limitations in our study. The retrospective study had some limitation in the contrast of imaging and pathological features. Because of the rigour inclusion criteria and single institution study, the sample size of study was unsatisfactory. However, we have done our best to overcome the shortage by inviting the rich experienced pathologists and radiologists to analyze the pathological records and CT findings. Further prospective large-sample study and logistic multivariate regression analysis are mandatory to find the potential indicators to VPI, even to predict the incidence of VPI.

Conclusions

Pleural signs of pulmonary adenocarcinoma can be categorized into five types of group A and four types of group B. The PIF value is firstly defined and that of type I in group B can be estimated by the equation of linear regression. The rate of VPI in type III,IV of group A and type I of group B are higher while the ratio of VPI in type III of group B is 2/2 which may be the indicators to VPI. Non-intact extrapleural fat layer and mediastinal pleural abnormality may increase the diagnosis accuracy of VPI in the basis of those pleural signs.

Acknowledgements

None.

Footnote

Conflicts of Interest: The authors have no conflicts of interest to declare.

Ethical Statement: The review board of Tongji medical college, Huazhong university of science and technology approved the protocol of this study (No. S254) and waived the requirement for patient informed consent.

References

1. Siegel RL, Miller KD, Jemal A. Cancer statistics, 2016. *CA Cancer J Clin* 2016;66:5-29.
2. Jemal A, Siegel R, Ward E, et al. Cancer statistics, 2009. *CA Cancer J Clin* 2009;59:225-49.
3. Detterbeck FC, Boffa DJ, Kim AW, et al. The Eighth Edition Lung Cancer Stage Classification. *Chest* 2017;151:193-203.
4. Zhao LL, Xie HK, Zhang LP, et al. Visceral pleural invasion in lung adenocarcinoma ≤ 3 cm with ground-glass opacity: a clinical, pathological and radiological study. *J Thorac Dis* 2016;8:1788-97.
5. Brewer LA. Patterns of survival in lung cancer. *Chest* 1977;71:644-50.
6. Manac'h D, Riquet M, Medioni J, et al. Visceral pleura invasion by non-small cell lung cancer: an underrated bad prognostic factor. *Ann Thorac Surg* 2001;71:1088-93.
7. Yang X, Soimakallio S. Pleural signs of small peripheral pulmonary masses: pathologic correlation with chest radiographs and diagnostic value. *Eur J Radiol* 1997;25:146-51.
8. Hsu JS, Han IT, Tsai TH, et al. Pleural Tags on CT Scans to Predict Visceral Pleural Invasion of Non-Small Cell Lung Cancer That Does Not Abut the Pleura. *Radiology* 2016;279:590-6.
9. Simon. Exeresis and extra-pleural pneumothorax in the treatment of pulmonary tuberculosis in children. *Rev Tuberc Pneumol (Paris)* 1961;25:1507-13.
10. Sone S, Sakai F, Takashima S, et al. Factors affecting the radiologic appearance of peripheral bronchogenic carcinomas. *J Thorac Imaging* 1997;12:159-72.
11. Wu HW, Xiao XS, Liu SY, et al. Intra-tumor basis and influential factors of pleural indentation in peripheral lung cancer (in Chinese). *Chin J Radiol* 2001;35:731-35.
12. Kawase A, Yoshida J, Ishii G, et al. Visceral pleural invasion classification in non-small cell lung cancer. *J Thorac Oncol* 2010;5:1784-8.
13. The Japanese Lung Cancer Society. General rule for clinical and pathological record of lung cancer. 7th edition. Tokyo: Kanehara, 2010.
14. Miura H, Taira O, Uchida O, et al. Invasion beyond interlobar pleura in non-small cell lung cancer. *Chest* 1998;114:1301-4.
15. Demir A, Gunluoglu MZ, Sansar D, et al. Staging and resection of lung cancer with minimal invasion of the adjacent lobe. *Eur J Cardiothorac Surg* 2007;32:855-8.
16. Verschakelen JA, Bogaert J, De Wever W. Computed tomography in staging for lung cancer. *Eur Respir J Suppl* 2002;35:40s-8s.
17. Kamiyoshihara M, Kawashima O, Sakata S, et al. Does

- an incomplete interlobar fissure influence survival or recurrence in resected non-small-cell lung cancer? *Lung Cancer* 1999;25:33-8.
18. Nomori H, Ohtsuka T, Horio H, et al. Thoracoscopic lobectomy for lung cancer with a largely fused fissure. *Chest* 2003;123:619-22.
19. Craig SR, Walker WS. A proposed anatomical classification of the pulmonary fissures. *J R Coll Surg Edinb* 1997;42:233-4.
20. Leung AN, Müller NL, Miller RR. CT in differential diagnosis of diffuse pleural disease. *AJR Am J Roentgenol* 1990;154:487-92.

Cite this article as: Yang S, Yang L, Teng L, Zhang S, Cui Y, Cao Y, Shi H. Visceral pleural invasion by pulmonary adenocarcinoma ≤ 3 cm: the pathological correlation with pleural signs on computed tomography. *J Thorac Dis* 2018;10(7):3992-3999. doi: 10.21037/jtd.2018.06.125